



Low-voltage blue-phase liquid crystal display with diamond-shape electrodes

Haiwei Chen^a, Yi-Fen Lan^b, Cheng-Yeh Tsai^b and Shin-Tson Wu^a

^aCollege of Optics and Photonics, University of Central Florida, Orlando, FL, USA; ^bAdvanced Display Technology Centre, AU Optronics Corp., Hsinchu, Taiwan

ABSTRACT

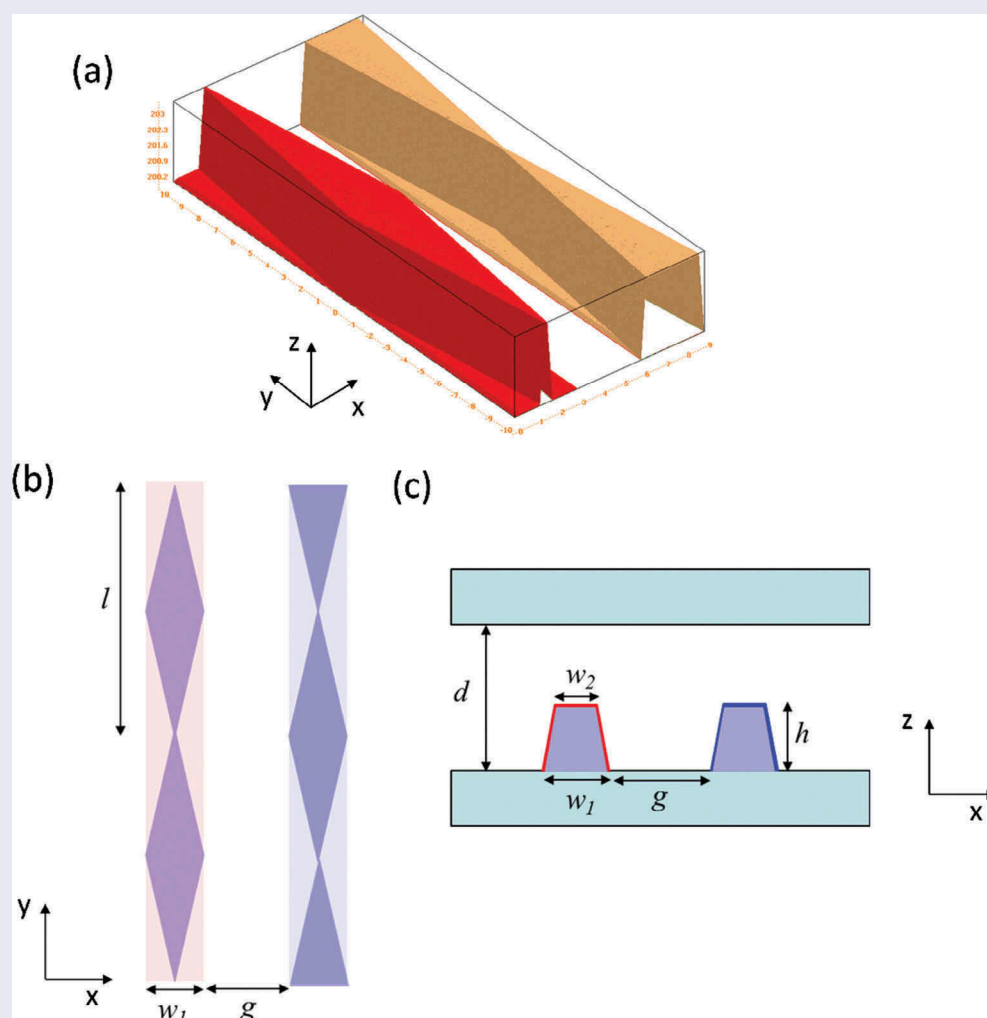
We propose a new electrode configuration, called diamond-shape in-plane switching, to lower the operation voltage of polymer-stabilised blue-phase liquid crystal (BPLC) displays (BPLCDs). The electrode structure is modified from conventional protruded IPS, where the strip protrusion is changed to diamond shape. By optimising the electrode gap and diamond length, we are able to obtain peak transmittance over 75% at 15 V. It enables single thin-film transistor (TFT) driving, and more importantly, this is based on an industrially proven BPLC material. That means good long-term stability, adequate TFT charging time for high-resolution displays and sub-millisecond response time and acceptable voltage-holding ratio for field sequential displays can be achieved simultaneously. Our device design helps accelerate the emergence of the long-awaited BPLCDs.

ARTICLE HISTORY

Received 6 November 2016
Accepted 20 November 2016

KEYWORDS

Liquid crystal display; blue phase; in-plane switching; protrusion electrodes



1. Introduction

Polymer-stabilised blue-phase liquid crystal (BPLC) is a strong contender for next-generation displays because it exhibits several outstanding features, such as sub-millisecond response time, no need for surface alignment, optically isotropic dark state and cell gap insensitivity [1–6]. Fast response time enables field sequential colour displays with negligible colour breakup [7–9]. By removing the red, green and blue colour filters, both optical efficiency and resolution density are tripled [10]. After about 15 years of extensive efforts, most of the problems impeding the commercialisation of BPLC have been gradually overcome, such as long-term stability, protrusion fabrication, slow TFT (thin-film transistor) charging time etc. [11,12]. However, the on-state voltage (V_{on}) is still too high to be addressed by a single TFT per pixel.

To lower operation voltage, enlarging the Kerr constant (K) of BPLC mixture seems to be a straightforward approach because $V_{on} \sim 1/\sqrt{K}$ [13]. Indeed, this is where material efforts have been devoted in the past few years [14,15]. Some high birefringence BPLC hosts with dielectric anisotropy $\Delta\epsilon > 100$ have been developed [13–16]. However, the major trade-offs for such a huge $\Delta\epsilon$ BPLC material are (1) increased response time (>1 ms) due to its high viscosity, (2) prolonged TFT charging time due to its large capacitance and (3) compromised long-term stability and voltage-holding ratio (VHR). For a high resolution and high frame rate (≥ 120 Hz) display, the maximum $\Delta\epsilon$ of the BPLC should not exceed 100. With that, slow charging issue can still be managed by the bootstrapping driving scheme [11,12], while its VHR could reach as high as 99%, depending on the charging time (governed by the frame rate and resolution density) and working temperature [15]. Moreover, its long-term stability has been verified experimentally, as reported in Ref. [14]. As a matter of fact, such a BPLC mixture ($\Delta\epsilon < 100$) has already been experimentally proven by AUO in a 10" prototype [17]. Indeed, its overall performance is quite impressive except that V_{on} is still as high as $32 V_{rms}$. As a result, two TFTs per pixel are required. The power consumption of a display driver IC (excluding backlight) is proportional to $(V_{on})^2$. Therefore, it is essential to lower the V_{on} to ≤ 15 V to enable single TFT driving with this practical BPLC material ($\Delta\epsilon \leq 100$). Such a burden falls on the new device structure.

In this paper, we propose a new protruded diamond-shape in-plane switching (DIPS) electrode configuration to lower the operation voltage. By optimising

the device parameters, we can boost the peak transmittance to over 75% at 15 V. It enables single-TFT driving and lower the power consumption, and more importantly, this is achieved using a practical BPLC material with mild $\Delta\epsilon$. We also investigate the zigzag two-domain structure for realising wide viewing angle and suppressing gamma shift to unnoticeable level. Our approach would undoubtedly accelerate the emergence of the long-awaited blue-phase liquid crystal displays (BPLCDs).

2. Structure design and working mechanism

The induced birefringence Δn_i of an optically isotropic BPLC can be described by the extended Kerr model [18]:

$$\Delta n_i(E) = \Delta n_s \left\{ 1 - \exp \left[- \left(\frac{E}{E_s} \right)^2 \right] \right\}, \quad (1)$$

where Δn_s stands for the saturated induced birefringence, E is the applied electric field and E_s represents the saturation field. However, above the electrode, the generated electric field is along vertical direction so that little phase retardation is produced, leading to low transmittance (known as dead zones). In order to boost transmittance, a large electrode gap is often employed, which in turn increases the operation voltage.

Figure 1(a) depicts the DIPS electrode structure. The conventional strip protrusion is modified to diamond shape (Figure 1(b)) so that the effective dead zone area can be greatly reduced. From the cross-section view (Figure 1(c)), it is almost the same as traditional protruded IPS [17,19]. Here, the electrode width and protrusion height are fixed as $w_1 = 3 \mu\text{m}$ and $h = 3.5 \mu\text{m}$, respectively, to be compatible with current fabrication technology [17]. As Figure 1 shows, there is a spatial shift between adjacent pixel and common electrodes. This helps boost the total transmittance, as will be discussed later.

From fabrication viewpoint, our DIPS structure shares the same procedures as conventional protruded IPS, as reported in Ref. [17]. Although we have not actually fabricated the DIPS device, its procedures are outlined as follows: The first step is to form diamond-shape protrusions (e.g. SiO_2 , Si_3N_4 , organic materials etc.) on the bottom substrate by photolithography. The width of top side (Figure 1) is controlled to be $w_2 = 2.5 \mu\text{m}$ and the protrusion height is $h = 3.5 \mu\text{m}$. The second step is to overcoat the protrusion surface with a thin indium tin oxide layer. A strong and deep

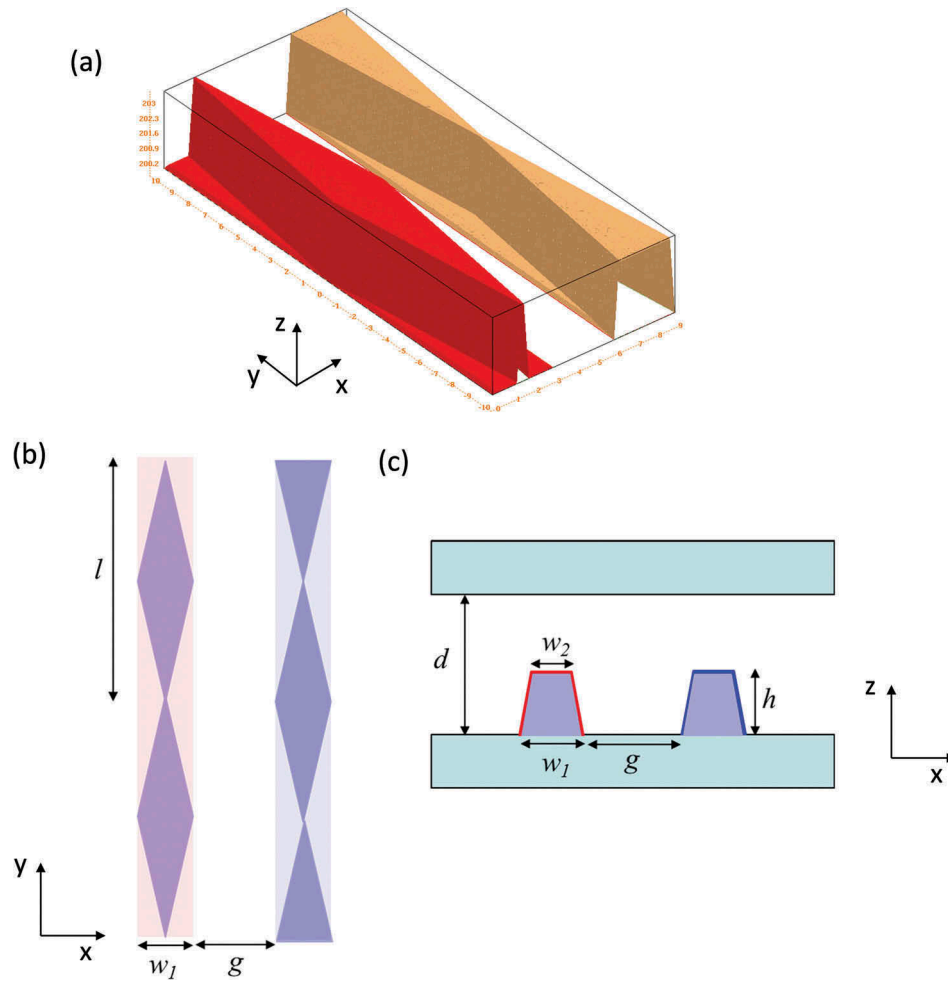


Figure 1. (a) Three-dimensional schematic diagram for DIPS; (b) top view and (c) cross-section view for DIPS.

penetrating horizontal electric field between the neighbouring electrodes is thus generated. No surface alignment layer is needed.

3. Simulation results

Next, we investigate the electro-optic performance of the proposed DIPS structure using a commercial software TechWiz LCD 3D (Sanayi, Korea). As discussed above, the protruded electrodes are designed with $w_1 = 3 \mu\text{m}$, $w_2 = 2.5 \mu\text{m}$ and $h = 3.5 \mu\text{m}$, which is compatible with current fabrication facility [17]. The electrode gap is set as $g = 3 \mu\text{m}$, and the cell gap is $d = 9 \mu\text{m}$. Another important factor is diamond length (l), which is assumed to be $20 \mu\text{m}$.

To obtain the BPLC parameters, we first fit the voltage-dependent transmittance (VT) curve reported by AUO, as Figure 2 shows, using Equation (1). Good agreement between experiment and simulation is obtained. The small difference is attributed to different

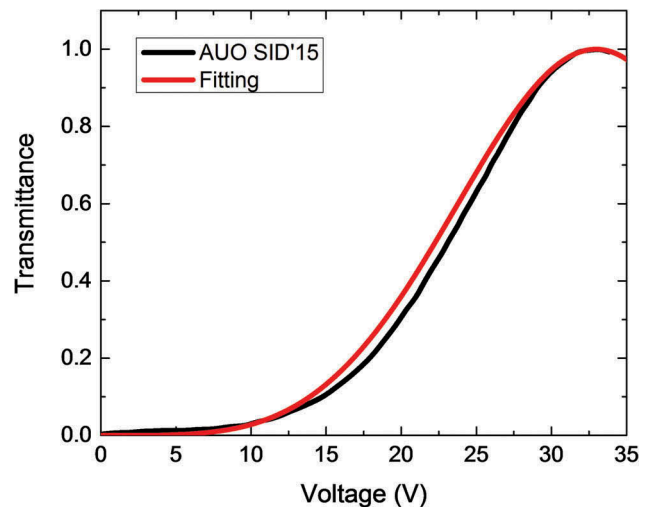


Figure 2. Numerical fitting for the VT curve reported in Ref. [16] using extended Kerr model ($\lambda = 550 \text{ nm}$).

light sources employed: for experiment, it is white light, while in our fitting, we use $\lambda = 550 \text{ nm}$. Through fitting, we obtained $\Delta n_s = 0.16$ and $E_s = 5.7 \text{ V}/\mu\text{m}$, which

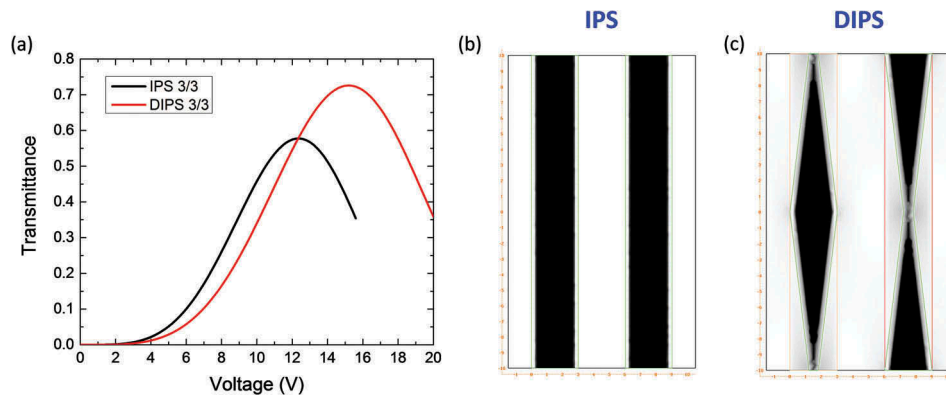


Figure 3. (Colour online) (a) Simulated VT curves for conventional protruded IPS and DIPS; brightness profile at on-state voltage for (b) conventional IPS and (c) DIPS ($w_1 = 3 \mu\text{m}$, $w_2 = 2.5 \mu\text{m}$, $g = 3 \mu\text{m}$, $h = 3.5 \mu\text{m}$ and $d = 9 \mu\text{m}$ for both IPS and DIPS. $l = 20 \mu\text{m}$ for DIPS only).

corresponds to $K = 9.28 \text{ nm/V}^2$ at $\lambda = 550 \text{ nm}$. From here on, we will use these BPLC material parameters in our device optimisation.

Figure 3(a) shows the simulated VT curves for conventional IPS and newly proposed DIPS. As expected, the peak transmittance of DIPS is much higher than that of IPS (72.6% vs. 57.8%), due to the reduced dead zone area. This effect could be virtualised more clearly from Figures 3(b,c). For conventional IPS, a large strip dead zone exists above the electrode, while for DIPS, the protrusion size is reduced, along with the reduced dark region. As a result, the transmittance is improved significantly. But the trade-off is slightly increased voltage (15.2 vs. 12.4 V), since the effective electrode gap is larger.

Next, we tune the electrode gap from 2.5 to 5 μm , and their corresponding VT curves are depicted in Figure 4. Both operation voltage and peak transmittance keep increasing as the electrode gap gets larger. If we set $V_{on} = 15 \text{ V}$, the highest transmittance (72.5%) is obtained when the electrode gap $g = 3 \mu\text{m}$. For further optimisations, we will keep $g = 3 \mu\text{m}$.

Due to the specially designed diamond shape, the generated electric field is not parallel to the x -axis;

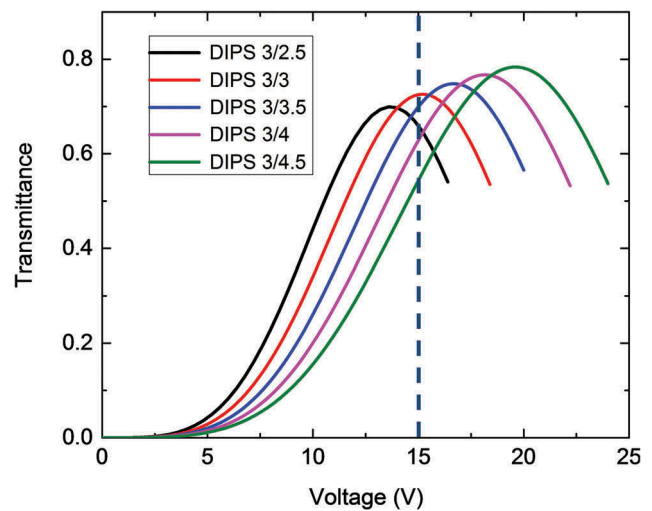


Figure 4. (Colour online) Simulated VT curves for different electrode gaps ($w_1 = 3 \mu\text{m}$, $w_2 = 2.5 \mu\text{m}$, $h = 3.5 \mu\text{m}$, $d = 9 \mu\text{m}$ and $l = 20 \mu\text{m}$).

instead, there is a small slanted angle (θ), as Figure 5 (a) shows. Therefore, the phase retardation is not fully utilised if the linear polariser is oriented at 45° with

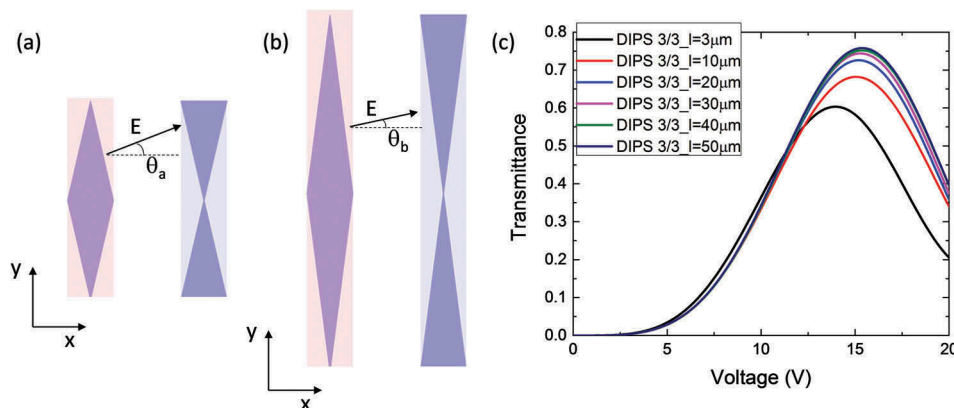


Figure 5. (Colour online) Schematic diagram for (a) short diamond electrode and (b) long diamond electrode; (c) simulated VT curves for different diamond lengths ($w_1 = 3 \mu\text{m}$, $w_2 = 2.5 \mu\text{m}$, $g = 3 \mu\text{m}$, $h = 3.5 \mu\text{m}$ and $d = 9 \mu\text{m}$).

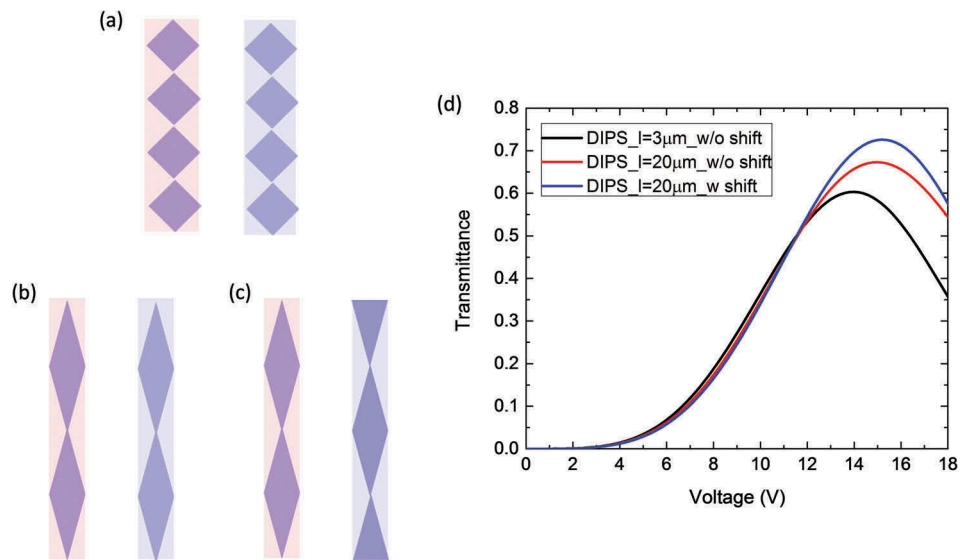


Figure 6. (Colour online) Schematic diagram for (a) un-shifted electrode with short diamond, (b) un-shifted electrode with long diamond, (c) shifted electrode with long diamond and (d) simulated VT curves for the structures in (a)–(c) ($w_1 = 3 \mu\text{m}$, $w_2 = 2.5 \mu\text{m}$, $g = 3 \mu\text{m}$, $h = 3.5 \mu\text{m}$ and $d = 9 \mu\text{m}$).

respect to x -axis. To reduce this slant angle, an efficient approach is to increase the diamond length (l). As it gets longer (Figure 5(b)), this angle gets smaller (i.e. $\theta_a > \theta_b$), leading to larger phase retardation. Figure 5(c) depicts the simulated VT curves as a function of diamond length. As expected, peak transmittance increases with l but gradually saturates when $l \geq 40 \mu\text{m}$. A similar trend is found for operation voltage: it increases first and then gradually saturates. Please note that when $l = 50 \mu\text{m}$, the transmittance at 15 V is as high as 75.5%, which is good enough for practical applications.

As Figure 6(c) shows, there is a spatial shift between adjacent pixel and common electrodes. In this case, the electric field is uniformly distributed. While for the un-shifted structures (Figures 6(a,b)), the generated electric field is distorted: stronger in the bulging region but weaker in the hollow region, resulting in a decreased transmittance. Figure 6(d) plots the simulated VT curves for these three cases, where the shifted configuration (Figure 6(c)) shows the highest transmittance. Its transmittance is 14.2% higher than that of un-shifted one with smaller diamond length, that is, square shape in Figure 6(a) [20].

4. Discussion

We investigate the electro-optic performance of DIPS structure and the influencing factors. With some optimisations, we have achieved 75.5% transmittance at 15 V. For conventional protruded IPS, it exhibits much larger dead zone (Figure 3(b)). As a result, to improve transmittance, a wider electrode gap

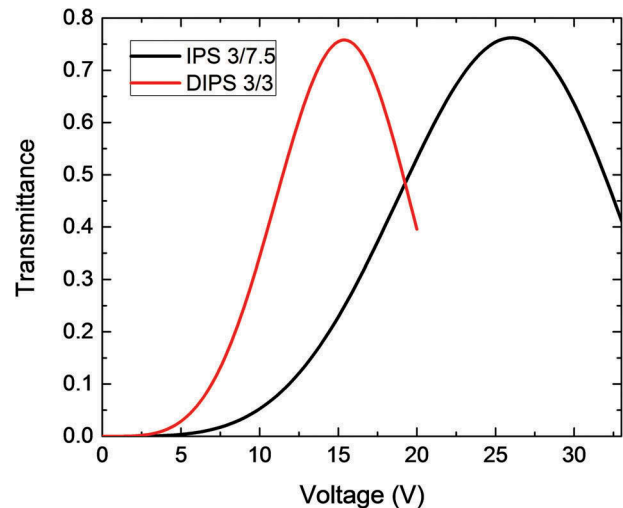


Figure 7. (Colour online) Simulated VT curves for conventional IPS and DIPS ($w_1 = 3 \mu\text{m}$, $w_2 = 2.5 \mu\text{m}$, $g = 7.5 \mu\text{m}$, $h = 3.5 \mu\text{m}$ and $d = 9 \mu\text{m}$ for IPS; $w_1 = 3 \mu\text{m}$, $w_2 = 2.5 \mu\text{m}$, $g = 3 \mu\text{m}$, $h = 3.5 \mu\text{m}$, $d = 9 \mu\text{m}$ and $l = 20 \mu\text{m}$ for DIPS).

($g = 7.5 \mu\text{m}$) is needed, which in turn increases the operation voltage (Figure 7). Compared to conventional protruded IPS, the on-state voltage of our DIPS is lowered by 41.4% (15.3 vs. 26.1 V) while keeping the same transmittance. Our design enables BPLCDs to be driven by a single TFT.

To obtain wide view and suppress gamma shifts, two-domain configuration is commonly employed [21]. Here, we simulate the performance of zigzag DIPS structure. Results are plotted in Figure 8. From Figure 8(a), the isocontrast ratio remains over 100:1 in

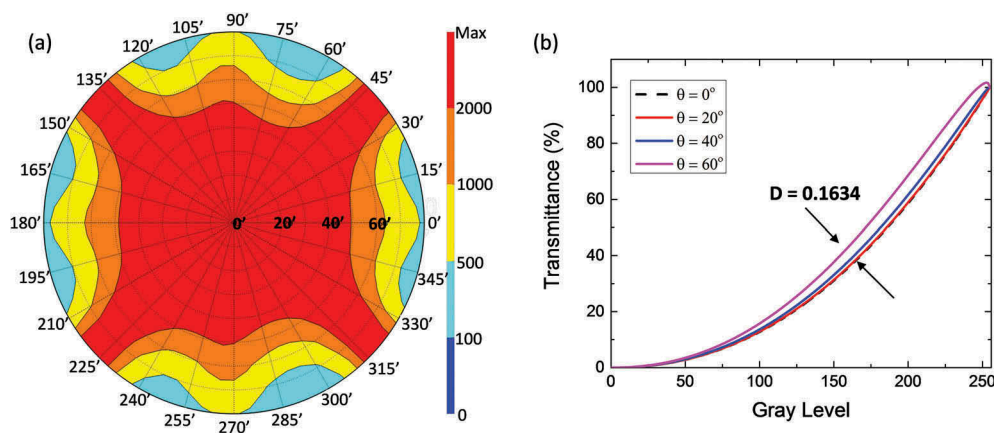


Figure 8. (a) Simulated isocontrast contour and (b) viewing angle dependence of gamma curves for biaxial film-compensated two-domain DIPS.

the entire viewing zone. Also, the calculated gamma shift (D) is only 0.1634, which is smaller than 0.2, that is, it is unnoticeable to the human eye [22,23]. Moreover, since we are using IPS structure, the electro-optic properties are insensitive to the cell gap [6]. Thus, BPLCD should work well for touch panels.

5. Conclusion

Our new diamond-shape protruded IPS structure helps to lower the operation voltage of a BPLCD to 15 V by using an industrially proven blue-phase material, while keeping a relatively high transmittance (75.5%). This is an important step towards enabling single-TFT driving using a practical BPLC material with a mild $\Delta\epsilon$ without compromising other desirable features, including sub-millisecond response time, long-term stability, no TFT charging issue, high VHR etc. As for the fabrications, DIPS shares the same fabrication process as conventional protruded IPS. Our DIPS structure would help to accelerate the emergence of the long-awaited blue-phase LCDs for widespread applications..

Acknowledgements

The authors would like to thank Fangwang Gou for helpful discussions. UCF group is indebted to a.u.Vista Inc. for the financial support.

Disclosure statement

No potential conflict of interest was reported by the authors

Funding

UCF group is indebted to a.u.Vista Inc. for the financial support.

References

- [1] Kikuchi H, Yokota M, Hisakado Y, et al. Polymer-stabilized liquid crystal blue phases. *Nat Mater.* 2002;1:64–68. DOI:10.1038/nmat712.
- [2] Kikuchi H, Higuchi H, Haseba Y, et al. 62.2: invited paper: fast electro-optical switching in polymer-stabilized liquid crystalline blue phases for display application. *SID Int Symp Digest Tech Pap.* 2007;38:1737–1740. DOI:10.1889/1.2785662.
- [3] Rao L, Ge Z, Wu ST, et al. Low voltage blue-phase liquid crystal displays. *Appl Phys Lett.* 2009;95:231101. DOI:10.1063/1.3271771.
- [4] Chen KM, Gauza S, Xianyu H, et al. Submillisecond gray-level response time of a polymer-stabilized blue-phase liquid crystal. *J Display Technol.* 2010;6:49–51. DOI:10.1109/JDT.2009.2037981.
- [5] Lee H, Park HJ, Kwon OJ, et al. The world's first blue phase liquid crystal display. *SID Int Symp Digest Tech Pap.* 2011;42:121–124. DOI:10.1889/1.3621051.
- [6] Ge Z, Rao L, Gauza S, et al. Modeling of blue phase liquid crystal displays. *J Display Technol.* 2009;5:250–256. DOI:10.1109/JDT.2009.2022849.
- [7] Hirakata Y, Kubota D, Yamashita A, et al. A novel field-sequential blue-phase-mode AMLCD. *J Soc Inf Disp.* 2012;20:38–46. DOI:10.1889/JSID20.1.38.
- [8] Ishitani T, Niikura Y, Ikenaga M, et al. High-performance polymer-stabilized blue-phase LCD with low driving voltage. *J Soc Inf Disp.* 2013;21:9–15. DOI:10.1002/jsid.152.
- [9] Cheng HC, Rao L, Wu ST. Color breakup suppression in field-sequential five-primary-color LCDs. *J Display Technol.* 2010;6:229–234. DOI:10.1109/JDT.2010.2042678.
- [10] Lin FC, Huang YP, Shieh HPD. Color breakup reduction by 180 Hz stencil-FSC method in large-sized color filter-less LCDs. *J Display Technol.* 2010;6:107–112. DOI:10.1109/JDT.2009.2027034.
- [11] Tu CD, Lin CL, Yan J, et al. Driving scheme using bootstrapping method for blue-phase LCDs. *J Display Technol.* 2013;9:3–6. DOI:10.1109/JDT.2012.2229694.
- [12] Lin CL, Tu CD, Cheng MH, et al. Novel dual-coupling pixel circuit to achieve high transmittance of blue-phase

- liquid crystal. *IEEE Electron Device Lett.* 2015;36:354–356. DOI:10.1109/LED.2015.2404973.
- [13] Rao L, Yan J, Wu ST, et al. A large Kerr constant polymer-stabilized blue phase liquid crystal. *Appl Phys Lett.* 2011;98:081109. DOI:10.1063/1.3559614.
- [14] Wittek M, Tanaka N, Wilkes D, et al. New materials for polymer-stabilized blue phase. *SID Int Symp Digest Tech Pap.* 2012;43:25–28. DOI:10.1002/j.2168-0159.2012.tb05699.x.
- [15] Haseba Y, Yamamoto SI, Sago K, et al. Low-voltage polymer-stabilized blue-phase liquid crystals. *SID Int Symp Digest Tech Pap.* 2013;44:254–257. DOI:10.1002/j.2168-0159.2013.tb06193.x.
- [16] Chen Y, Xu D, Wu ST, et al. A low voltage and sub-millisecond-response polymer-stabilized blue phase liquid crystal. *Appl Phys Lett.* 2013;102:141116. DOI:10.1063/1.4802090.
- [17] Tsai CY, Yu FC, Lan YF, et al. A novel blue phase liquid crystal display applying wall-electrode and high driving voltage circuit. *SID Int Symp Digest Tech Pap.* 2015;46:542–544. DOI:10.1002/sdtp.10466.
- [18] Yan J, Cheng HC, Gauza S, et al. Extended Kerr effect of polymer-stabilized blue-phase liquid crystals. *Appl Phys Lett.* 2010;96:071105. DOI:10.1063/1.3318288.
- [19] Yoon S, Kim M, Kim SM, et al. Optimisation of electrode structure to improve the electro-optic characteristics of liquid crystal display based on the Kerr effect. *Liq Cryst.* 2010;37:201–208. DOI:10.1080/02678290903494601.
- [20] Yamamoto T, Ikenaga M, Yamashita A, et al. Crystalline OS-LCD using blue-phase liquid crystal having characteristic texture. *SID Int Symp Digest Tech Pap.* 2012;43:201–204. DOI:10.1002/j.2168-0159.2012.tb05747.x.
- [21] Rao L, Ge Z, Wu ST. Zigzag electrodes for suppressing the color shift of Kerr effect-based liquid crystal displays. *J Display Technol.* 2010;6:115–120. DOI:10.1109/JDT.2009.2039463.
- [22] Kim SS, Berkeley BH, Kim KH, et al. New technologies for advanced LCD-TV performance. *J Soc Inf Disp.* 2004;2004(12):353–359. DOI:10.1889/1.1847732.
- [23] Gao YT, Luo ZY, Zhu RD, et al. A high performance single-domain LCD with wide luminance distribution. *J Display Technol.* 2015;11:315–324. DOI:10.1109/JDT.2015.2408993.